

Thermal phase transitions in the attractive extended Bose-Hubbard Model with three-body constraint

Kwai-Kong Ng* and Min-Fong Yang

Department of Physics, Tunghai University, Taichung 40704, Taiwan

(Dated: March 24, 2011)

By means of quantum Monte Carlo simulations implemented with a two-loop update scheme, the finite-temperature phase diagram of a three-body constrained attractive Bose lattice gas is investigated. The nature of the thermal phase transitions around the dimer superfluid and the atomic superfluid is unveiled. We find that the Z_2 symmetry-breaking transitions between these two superfluid phases are of first order even at nonzero temperatures. More interestingly, the thermal transition from the dimer superfluid to the normal fluid is found to be consistent with the Kosterlitz-Thouless type but giving an anomalous universal stiffness jump. It demonstrates that this transition is driven by unbinding of pairs of fractional vortices.

Since the early proposals of possible pair superfluidity in an attractive Bose gas,¹ the existence of this state of matter at low temperatures has been intensively explored.^{2,3} Recent developments on the manipulation of ultracold gases may provide direct routes in the search for the pair superfluid phase and in probing quantum critical behaviors around this intriguing state. In the context of Bose gases in the continuum, the possibility of observing such a pair superfluid phase near a Feshbach resonance has been proposed.⁴⁻⁷ Another realization in attractive bosonic lattice gases with three-body on-site constraint is also suggested recently.⁸ While the discussions of this pair condensed state was originally focused on the system of bosonic particles, similar physics can be applied to explain some exotic phases in other physical systems. For example, the quantum spin nematic state in some frustrated spin systems can be understood as the condensate state of bound magnon pairs.^{9,10}

The pair superfluid phase or the dimer superfluid (DSF) phase consists in the formation of a macroscopic coherent state made of boson pairs. Here we focus on the case of single-species bosons. Contrast to the conventional atomic superfluid (ASF) with non-vanishing order parameters $\langle a \rangle \neq 0$ and $\langle a^2 \rangle \neq 0$ (here a denotes the boson annihilation operator), DSF is characterized by the vanishing of atomic order parameter ($\langle a \rangle = 0$) but nonzero pairing correlation ($\langle a^2 \rangle \neq 0$). Apart from the above local order parameters, one can use superfluid stiffness to identify the superfluid states. It is expected that, in the DSF phase, pairs of bosons will wind together around the system, such that only even numbers of winding can occur. Hence the DSF phase can also be characterized by a nonzero pair superfluid stiffness given by even winding numbers $\rho_{\text{even}} \neq 0$ and a zero stiffness corresponding to odd winding numbers $\rho_{\text{odd}} = 0$ [see Eq. (2)].¹¹ Such an even-odd effect will not appear in the ASF phase. From the symmetry-breaking perspective, the $U(1)$ symmetry of the global phase transformation $a \rightarrow e^{i\varphi}a$ is completely broken in the ASF phase, while a residual Z_2 discrete symmetry remains in the DSF phase due to the π -periodicity of $\langle a^2 \rangle$. As a result, there should exist an Ising-like quantum phase transition be-

tween these two phases upon tuning system parameters. Nevertheless, as pointed out in Refs. 5–8, quantum fluctuations can turn this transition into a first-order one due to the Coleman-Weinberg mechanism.¹² Although there are many theoretical investigations on the existence of the DSF phase at zero temperature and on the nature of the related quantum phase transitions,^{4-8,13,14} reliable quantitative predictions, especially for the DSF-ASF transition, have not yet been provided except for the one-dimensional case.¹⁴ Moreover, the physics of the thermal transitions out of the DSF phase has neither been addressed.

In the present work, the nature of the finite-temperature phase transitions around the DSF phase in attractive bosonic lattice gases with three-body on-site constraint⁸ is explored numerically. We employ here the stochastic series expansion (SSE) Monte Carlo method¹⁵ generalized by allowing pair updates such that two independent loops can merge and move together. The importance of two-loop (or two-worm) algorithms for efficient sampling of the DSF phase (or any paired phase) in large system sizes has been discussed in the literature.^{11,16-19} Our results for the phase diagram are summarized in Fig. 1. The existence of the DSF phase characterized by the even-odd effect of the stiffness is confirmed in our simulations. Besides, it is found that the Z_2 symmetry-breaking transitions between the DSF and the ASF phases are still of first order at finite temperatures. This indicates that the underlying Coleman-Weinberg mechanism for the DSF-ASF transition at zero temperature is not completely spoiled by the thermal fluctuations. As for the transitions to normal fluids (N), both the DSF-N and the ASF-N transitions are found to be of continuous Kosterlitz-Thouless (KT) type.²⁰ Remarkably, these two KT transitions have distinct characters. Our data support an anomalous value of universal stiffness jump at the KT transition out of the DSF phase, which is *four times larger* than that out of the ASF phase. This observation clearly establishes that the DSF-N transition is driven by the proliferation of unconventional topological defects (half-vortices). Thus the anomalous stiffness jump can serve as a unique signature for the

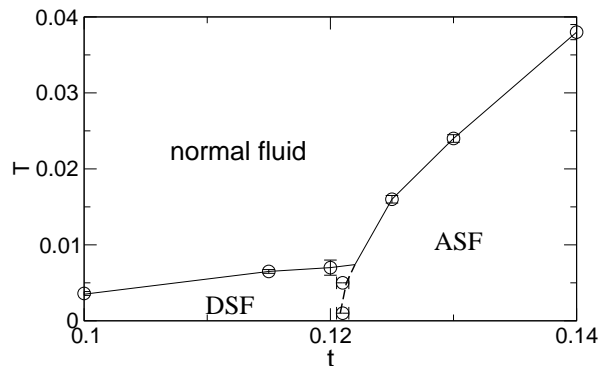


FIG. 1: Finite-temperature phase diagram of a three-body constrained attractive Bose gas on a square lattice as described in Eq. (1) with $|U| = 1$, $V = 0.25$, and $\mu = -0.55$. The solid lines indicate the DSF-N and ASF-N transitions of continuous KT type, and the dashed line shows the first-order DSF-ASF transition. Lines are guide to eyes.

search of the DSF phase in experiments.

We consider the following extended Bose-Hubbard model with a three-body constraint $a_i^{\dagger 3} \equiv 0$,

$$H = -t \sum_{\langle i,j \rangle} a_i^\dagger a_j + \frac{U}{2} \sum_i n_i (n_i - 1) + V \sum_{\langle i,j \rangle} n_i n_j - \mu \sum_i n_i. \quad (1)$$

Here, $a_i (a_i^\dagger)$ is the bosonic annihilation (creation) operator at site i , t is the hopping matrix element, $U < 0$ the on-site two-body attraction, and μ the chemical potential. $V > 0$ denotes the nearest-neighbor repulsion, which can come from the dipole-dipole interactions of the dipolar bosons polarized perpendicularly to the lattice plane by truncating it off at the nearest-neighbor distance. The convention $\langle i, j \rangle$ signifies a sum over nearest-neighbor sites i and j . The on-site constraint can arise naturally due to large three-body loss processes,²¹ and it stabilizes the attractive bosonic system against collapse. The intriguing quantum critical behaviors for $V = 0$ at zero temperature have been explored in Refs. 8,13. Here we consider a finite repulsive V which is found (not shown here) to stabilize the DSF phase and extend the region of this phase to larger t . It thus facilitates the access of the DSF phase in our simulations, and may also allow easy observation in the real experiments as well. We have also confirmed the same behaviors of the DSF for $V = 0$. As an illustration, we choose the parameters $V = 0.25$ and $\mu = -0.55$ ($|U| \equiv 1$ as the energy unit), so that the boson densities are always smaller than half-filling.

To characterize different phases, several kinds of superfluid stiffness are evaluated. In SSE, the conventional superfluid density ρ_s at temperature T is computed by measuring the fluctuation of the winding number W within the simulations,^{15,22} $\rho_s = mT \langle W^2 \rangle$. Here $m \equiv 1/2t$ is the effective mass of the bosons in a square lattice. If

a macroscopic fraction of the bosons winds around the system, the system will give a finite ρ_s . In the ASF phase, the usual algorithm is able to let a large number of bosons wind around the system and is known to be efficient. However, in the DSF phase, bosons are paired into dimers and hop together as pairs. Therefore only even winding numbers can occur. If we define the superfluid stiffness $\rho_{\text{even (odd)}}$ with respect to the even (odd) winding number $W_{\text{even (odd)}}$ in the following way:

$$\rho_{\text{even (odd)}} = mT \langle (W_{\text{even (odd)}})^2 \rangle, \quad (2)$$

then a clear even-odd effect, where $\rho_s = \rho_{\text{even}} \neq 0$ and $\rho_{\text{odd}} = 0$, should be observed in the DSF phase.¹¹ It is worth to note that there is no pair hopping term in the Hamiltonian H , so that the motion of boson pairs is manifested as a second-order effect in the single-particle hopping parameter t . Within the conventional one-loop updates of the SSE simulations, the boson numbers can only be varied by one during each vertex update. Here in our two-loop algorithm, the pair updates that change the boson number by two are included. As a consequence, two independent loops can merge and move together in such a way that effectively simulates the pair hopping in the DSF phase. Because the accumulation of a large number of winding boson pairs is exponentially suppressed by the short-range nature of the usual one-loop updates, the two-loop update scheme is necessary to improve the efficiency of the algorithm in finding the DSF phase.

As pointed out in Ref. 8, when the attraction U is strong enough, pairing correlation among bosons can be nonzero such that the system locates in a DSF phase. Conversely, by lowering the ratio of $|U|/t$, the ASF state can be stabilized. Thus there is a transition separating the DSF and the ASF phases. At zero temperature, this Z_2 symmetry-breaking transition is shown to be of first order in most conditions.⁸ By performing quantum Monte Carlo simulations to study the model in Eq. (1) on square lattices of size $N_s = L \times L$ under periodic boundary conditions, we find that this conclusion is still true at low temperatures. The results of various kinds of superfluid stiffness defined above as functions of the hopping parameter t at temperature $T = 0.005$ with system size $L = 48$ are shown in Fig. 2. It is found that, $\rho_s \simeq \rho_{\text{even}} \neq 0$ and $\rho_{\text{odd}} = 0$ for smaller hopping parameters, whereas for larger hopping parameters $\rho_s \simeq 2\rho_{\text{odd}} \neq 0$ and there is no even-odd effect. This indicates a transition from the DSF with $\rho_{\text{odd}} = 0$ to the ASF with nonzero ρ_{odd} . As seen from the lower panels of Fig. 2, upon increasing system sizes, ρ_{odd} shows an abrupt jump at $t = t_c \simeq 0.121$. It implies that the DSF-ASF transition remains being of first order at finite temperatures. To further exclude the possibility of a second-order transition, we have performed a finite-size scaling by assuming the critical exponents of the Ising universality class. The data of different system sizes do fail to collapse into a universal curve. This again advocates that the DSF-ASF transition should be of first order. Same conclusion about the nature of the DSF-ASF transition

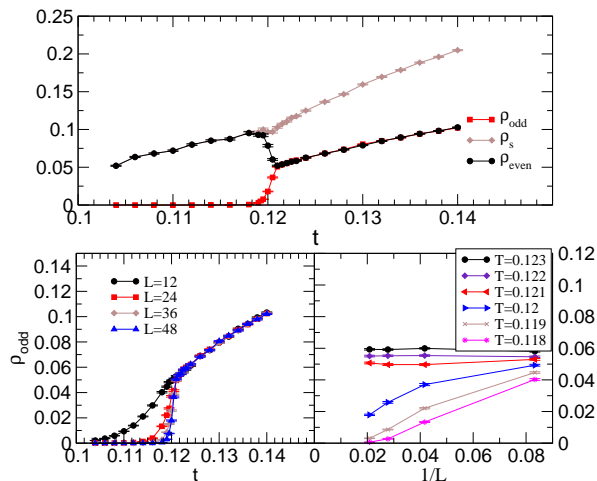


FIG. 2: (Color online) Upper panel: several kinds of superfluid stiffness as functions of t at $T = 0.005$ with system size $L = 48$. Lower panels: data of ρ_{odd} for different system sizes are shown to demonstrate the finite size effects. All error bars are smaller than the symbol size if not shown.

is reached for lower temperature $T = 0.001$.

As seen in Fig. 1, increasing temperature further, either the DSF or the ASF order will be eventually destroyed by thermal fluctuations, and will undergo a symmetry-restoration transition to the normal-fluid state. Before presenting the detailed analysis of these transitions, let's begin with discussions on some general aspects of their nature. While both the DSF-N and the ASF-N transitions are expected to be the continuous KT transitions, there is an essential difference between them. Because the DSF phase preserves the π phase-rotation symmetry, it can be characterized by an algebraic order in $\exp(2i\theta)$ rather than in $\exp(i\theta)$, where θ is the superfluid phase. Therefore, the KT transition out of the DSF phase should consist in proliferating of pairs of fractional vortices with vorticity $\nu = \pm 1/2$, instead of the ordinary (integer) vortices. As a result, the strength of the logarithmic interaction of these fractional vortices will be reduced by a factor of $\nu^2 = 1/4$ in comparison with that of integer vortices, and the KT transition temperature T_{KT} will be decreased substantially. The universal jump of the superfluid stiffness at such KT transitions driven by unbinding of fractional vortices has an anomalous value,²³ $\rho_s = (2/\pi\nu^2)mT_{\text{KT}}$, which amounts to $\rho_s = 8mT_{\text{KT}}/\pi$ for vorticity $\nu = \pm 1/2$. The existence of an anomalous KT transition has been proposed in other physical systems.^{23,24}

It is known that the KT transition temperatures can be determined with good accuracy by utilizing the renormalization flow and the universal jump of the superfluid density at the transition point.^{25,26} Here we generalize the data analysis suggested in Ref. 26 to take into account the anomalous superfluid stiffness jump. Consistent results can be reached by other kinds of analysis. Define $R \equiv \pi\nu^2\rho_s/2mT$ such that $R = 1$ at the KT transition

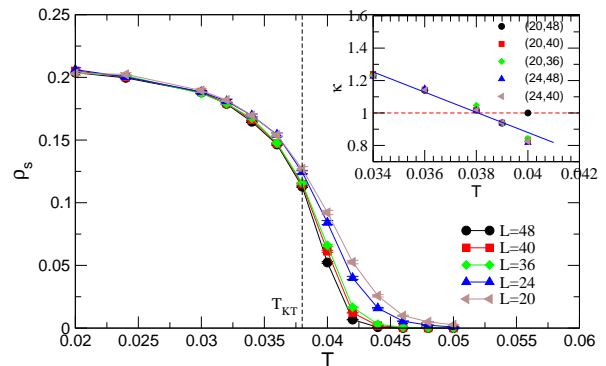


FIG. 3: (Color online) Superfluid density ρ_s vs temperature T with different system sizes for $t = 0.14$. The dash line denotes the location of T_{KT} . Inset: solutions of the Eq. (3) for different pairs of system sizes (L_1, L_2) for $R = \pi\nu^2\rho_s/2mT$ with $\nu = 1$. The blue solid line is the linear fit $\kappa = 1 + 8.71(T_{\text{KT}} - T)/t$ with $T_{\text{KT}} \simeq 0.038$ and the red dash line is $\kappa = 1$.

temperature T_{KT} . It is known that the KT renormalization group equations can be cast into an integral form,

$$4 \ln(L_2/L_1) = \int_{R_2}^{R_1} \frac{dt}{t^2(\ln(t) - \kappa) + t}, \quad (3)$$

where the parameter κ is an analytic function of temperature, and the temperature giving $\kappa = 1$ corresponds to the KT transition point. For $T < T_{\text{KT}}$, a linear function in $(T_{\text{KT}} - T)$ is expected, that is, $\kappa(T) \simeq 1 + c(T_{\text{KT}} - T)$ with a positive slope c .²⁶ Thus, after taking different pairs of system sizes in Eq. (3) at each temperature to determine the $\kappa(T)$ curve, the location of the KT transition temperature can be achieved by finding $\kappa(T_{\text{KT}}) = 1$.

Our findings of the superfluid density ρ_s as a function of temperature T for $t = 0.14$ are depicted in Fig. 3. We can see the strong system size dependence characteristic to the KT transition especially around and above the critical temperature. As seen from Figs. 1 and 2, the low-temperature states at this hopping parameter belong to the ASF phase. Thus the conventional KT transition driven by unbinding of ordinary (integer) vortices is expected. The results of the parameter κ in Eq. (3) with $\nu = 1$ for R are shown in the inset of Fig. 3. The values of $\kappa(T)$ extracted from various pairs of system sizes clearly collapse into a straight line around the value of $\kappa = 1$. This smooth analytic behavior of $\kappa(T)$ supports that the transition is of the usual KT type. Besides, the KT transition temperature is found to be $T_{\text{KT}} \simeq 0.038$. Thus the corresponding universal stiffness jump in the thermodynamic limit is $\rho_s = 2mT_{\text{KT}}/\pi \simeq 0.086$.

As discussed above, the low-temperature states for small hopping parameter t can be in the DSF phase, and the anomalous KT transition driven by unbinding of half-vortices ($\nu = \pm 1/2$) should be observed when temperature is increased. As an illustration, our results of ρ_s vs T for $t = 0.1$, where the system stays in the DSF phase at low temperatures, are shown in the left panel of Fig. 4. Similar to the previous data analysis but using $\nu = 1/2$

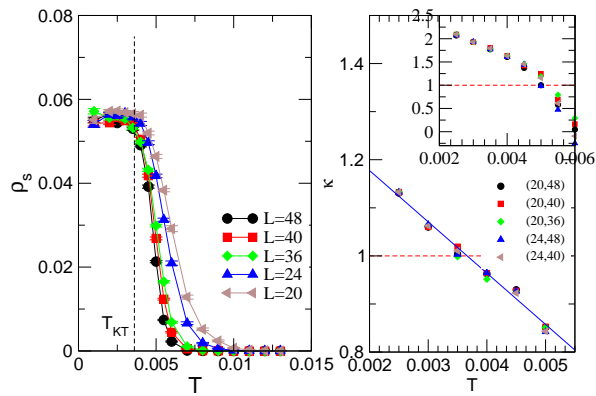


FIG. 4: (Color online) Left panel: superfluidity stiffness ρ_s vs T with different system sizes for $t = 0.1$. The dash line denotes the location of T_{KT} . Right panel: solutions of the Eq. (3) for different pairs of system sizes (L_1, L_2) for $R = \pi\nu^2\rho_s/2mT$ with $\nu = 1/2$. The blue solid line is the linear fit $\kappa = 1 + 10.67(T_{KT} - T)/t$ with $T_{KT} \simeq 0.0036$ and the red dash line is $\kappa = 1$. The inset shows the same analysis but using $\nu = 1$ for R .

for R , the results of $\kappa(T)$ are presented in the right panel of Fig. 4. Again, the data collapse is evident, supporting that this transition is of the KT type, but originated from the unbinding of half-vortices. For comparison, we repeat the same analysis with $\nu = 1$ for R , as presented in the inset of the right panel of Fig. 4. Data collapse becomes poor around the value of $\kappa = 1$, and $\kappa(T)$ does not behave as a linear function in $(T_{KT} - T)$ for $T < T_{KT}$. These observations eliminate the possibility of the conventional KT transition. Therefore, our findings offer strong evidences of the existence of a half-vortex unbinding transition out of the DSF phase and also serve as a

clear signature of the DSF phase itself. From Fig. 4, we observe that the KT transition happens at $T_{KT} \simeq 0.0036$, which is about one order less than the value for the case of $t = 0.14$. The corresponding stiffness jump for $t = 0.1$ in the thermodynamic limit is $\rho_s = 8mT_{KT}/\pi \simeq 0.046$, which is again less than the value for $t = 0.14$.

In our simulations, the above conclusions about the nature of the DSF-N and the ASF-N transitions apply also to the corresponding cases with the chosen t 's as presented in Fig. 1. This implies that, if it exists, the possible region of the superfluid-to-normal-fluid transitions of types different from the KT transition should be very narrow.

In summary, we study the DSF and the ASF phases in the extended Bose-Hubbard model with a three-body constraint and identify the nature of the related thermal phase transitions. The even-odd effect in the stiffness distinguishes the DSF from the ASF phase. The transition between these two superfluid phases is found to be of first order. More importantly, the DSF-N transition is shown to be driven by the topological defects of half-vortices, in great contrast to the conventional ASF-N transition. Stimulated by the recent progress on detecting the KT transitions in cold atom,²⁷ our predictions may be verified in the near future.

We are grateful to Y.-C. Chen for enlightening discussions and earlier collaborations. K.-K. Ng and M.-F. Yang thank the support from the National Science Council of Taiwan under grant NSC 97-2112-M-029-003-MY3 and NSC 99-2112-M-029-003-MY3, respectively. After the submission of this paper we became aware of a parallel numerical work²⁸ for the case of $V = 0$, which reaches similar conclusions.

* Electronic address: kknng@thu.edu.tw

¹ J. G. Valatin and D. Butler, *Nuovo Cimento* **10**, 37 (1958).
² W. A. B. Evans and Y. Imry, *Nuovo Cimento B* **63**, 155 (1969); P. Nozières and D. Saint James, *J. Phys. (Paris)* **43**, 1133 (1982).
³ M. J. Rice and Y. R. Wang, *Phys. Rev. B* **37**, 5893 (1988); M. Yu. Kagan and D. V. Efremov, *Phys. Rev. B* **65**, 195103 (2002).
⁴ L. Radzihovsky, J. I. Park, and P. B. Weichman, *Phys. Rev. Lett.* **92**, 160402 (2004); M. W. J. Romans, R. A. Duine, S. Sachdev, H. T. C. Stoof, *Phys. Rev. Lett.* **93**, 020405 (2004).
⁵ Y.-W. Lee and Y.-L. Lee, *Phys. Rev. B* **70**, 224506 (2004).
⁶ K. Sengupta and N. Dupuis, *Europhys. Lett.* **70**, 586 (2005).
⁷ L. Radzihovsky, P. B. Weichman, and J. I. Park, *Ann. Phys.* **323**, 2376 (2008).
⁸ S. Diehl, M. Baranov, A. J. Daley, and P. Zoller, *Phys. Rev. Lett.* **104**, 165301 (2010); *Phys. Rev. B* **82**, 064509 (2010); *Phys. Rev. B* **82**, 064510 (2010).
⁹ N. Shannon, T. Momoi, and P. Sindzingre, *Phys. Rev. Lett.*

96, 027213 (2006).
¹⁰ M. E. Zhitomirsky and H. Tsunetsugu, *Europhys. Lett.* **92**, 37001 (2010), and references therein.
¹¹ K. P. Schmidt, J. Dorier, A. Läuchli, and F. Mila, *Phys. Rev. B* **74**, 174508 (2006).
¹² S. Coleman and E. Weinberg, *Phys. Rev. D* **7** 1888 (1973); B. I. Halperin, T. C. Lubensky, and S.-K. Ma, *Phys. Rev. Lett.* **32**, 292 (1974).
¹³ Y.-W. Lee and M.-F. Yang, *Phys. Rev. A* **81**, 061604(R) (2010).
¹⁴ V. G. Rousseau and P. J. H. Denteneer, *Phys. Rev. Lett.* **102**, 015301 (2009); M. Eckholt and T. Roscilde, *Phys. Rev. Lett.* **105**, 199603 (2010); S. Ejima, M. J. Bhaseen, M. Hohenadler, F. H. L. Essler, H. Fehske, and B. D. Simons, *Phys. Rev. Lett.* **106**, 015303 (2011).
¹⁵ A. W. Sandvik, *Phys. Rev. B* **56**, 11678 (1997); *Phys. Rev. B* **59**, R14157 (1999); O. F. Syljuåsen and A. W. Sandvik, *Phys. Rev. E* **66**, 046701 (2002).
¹⁶ L. Pollet, M. Troyer, K. Van Houcke, and S. M. A. Rombouts, *Phys. Rev. Lett.* **96**, 190402 (2006).
¹⁷ S. Guertler, M. Troyer, and F.-C. Zhang, *Phys. Rev. B* **77**,

- 184505 (2008).
- ¹⁸ Ş. G. Söyler, B. Capogrosso-Sansone, N. V. Prokof'ev, and B. V. Svistunov, *New J. Phys.* **11**, 073036 (2009).
- ¹⁹ T. Ohgoe and N. Kawashima, arXiv:1009.3555.
- ²⁰ J. M. Kosterlitz and D. J. Thouless, *J. Phys. C* **6**, 1181 (1973).
- ²¹ A. J. Daley, J. M. Taylor, S. Diehl, M. Baranov, and P. Zoller, *Phys. Rev. Lett.* **102**, 040402 (2009); M. Roncaglia, M. Rizzi, and J. I. Cirac, *Phys. Rev. Lett.* **104**, 096803 (2010).
- ²² E. L. Pollock and D. M. Ceperley, *Phys. Rev. B* **36**, 8343 (1987).
- ²³ S. E. Korshunov, *Phys. Rev. B* **65**, 054416 (2002).
- ²⁴ S. Mukerjee, C. Xu, and J. E. Moore, *Phys. Rev. Lett.* **97**, 120406 (2006).
- ²⁵ H. Weber and P. Minnhagen, *Phys. Rev. B* **37**, 5986 (1988).
- ²⁶ M. Boninsegni and N. Prokof'ev, *Phys. Rev. Lett.* **95**, 237204 (2005).
- ²⁷ L. Hung, X. Zhang, N. Gemelke and C. Chin, *Nature* **470**, 236 (2011), and references therein.
- ²⁸ L. Bonnes and S. Wessel, arXiv:1101.5991.